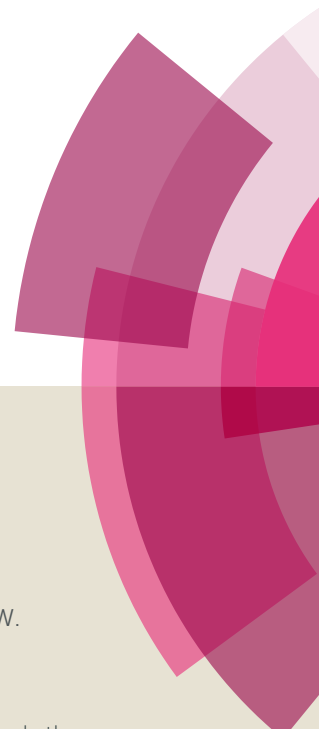


MedChemComm

Accepted Manuscript



This article can be cited before page numbers have been issued, to do this please use: P. Li, H. Jiang, W. Zhang, Y. Li, C. Dong, H. Chen, K. Zhang and Z. Du, *Med. Chem. Commun.*, 2018, DOI: 10.1039/C8MD00278A.



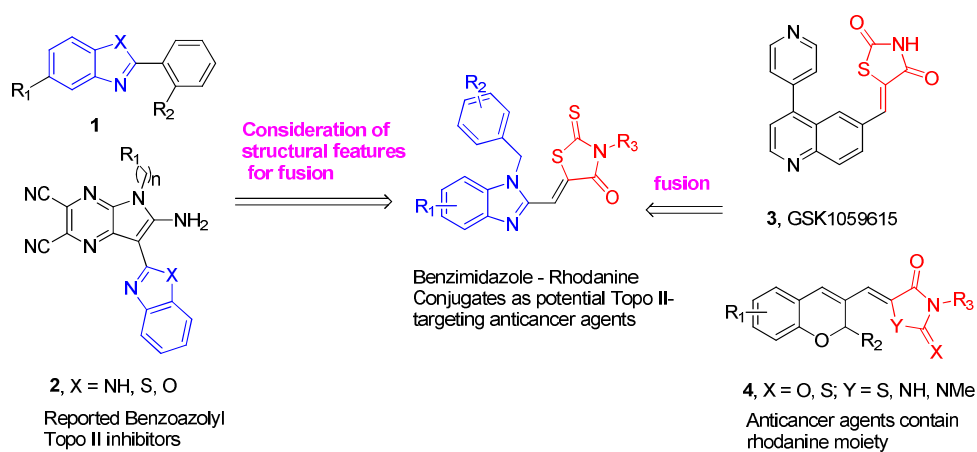
This is an Accepted Manuscript, which has been through the Royal Society of Chemistry peer review process and has been accepted for publication.

Accepted Manuscripts are published online shortly after acceptance, before technical editing, formatting and proof reading. Using this free service, authors can make their results available to the community, in citable form, before we publish the edited article. We will replace this Accepted Manuscript with the edited and formatted Advance Article as soon as it is available.

You can find more information about Accepted Manuscripts in the [author guidelines](#).

Please note that technical editing may introduce minor changes to the text and/or graphics, which may alter content. The journal's standard [Terms & Conditions](#) and the ethical guidelines, outlined in our [author and reviewer resource centre](#), still apply. In no event shall the Royal Society of Chemistry be held responsible for any errors or omissions in this Accepted Manuscript or any consequences arising from the use of any information it contains.

Table of contents



Title page**Design, synthesis and biological evaluation of benzimidazole-rhodanine conjugates as potent topoisomerase II inhibitors**

Penghui Li^a, Wenjin Zhang^a, Hong Jiang^a, Yongliang Li^a, Changzhi Dong^{a,b}, Huixiong Chen^{a,c}, Kun Zhang^{a,d}, Zhiyun Du^{a*}

^a*Institute of Natural Medicine & Green Chemistry, School of Chemical Engineering and Light Industry, Guangdong University of Technology, Guangzhou 510006, China*

^b*Universite Paris Diderot, Sorbonne Paris Cite, ITODYS, UMR 7086 CNRS, 15 rue J-A de Baif, 75270 Cedex 13 Paris, France*

^c*CNRS, UMR8601, Laboratoire de Chimie et Biochimie Pharmacologiques et Toxicologiques, CBNIT, Universite Paris Descartes PRES Sorbonne Paris Cite, UFR Biomedicale, 45 rue des Saints-Peres, 75270 Cedex 06 Paris, France.*

^d*Wuyi University, Jiangmen 529020, China.*

*Corresponding authors:

E-mail addresses: zhiyundu@gdut.edu.cn (Z. Y. Du).

Abstract

In this study, a series of benzimidazole-rhodanine conjugates were designed, synthesized and investigated for their topoisomerase II (Topo II) inhibition and cytotoxic activities. The results from Topo II-mediated pBR322 DNA relaxation and cleavage assay showed that the synthesized compounds might act as Topo II catalytic inhibitors. Certain compounds displayed potent Topo II inhibition at 10 μ M. The cytotoxic activities against HeLa, A549, Raji, PC-3, MDA-MB-201, and HL-60 cancer cell lines of these compounds were evaluated. The results indicated that these compounds exhibited strong antiproliferation activity. A good relationship was observed between the Topo II inhibition potency and the cytotoxicity of these compounds. The structure-activity relationship revealed that the electronic effects, the phenyl group, and the rhodanine moiety were particularly important for the Topo II inhibition potency and cytotoxicity.

Keywords

Benzimidazole

Rhodanine

Topoisomerase

Anticancer

Pharmacophore hybridization strategy

1. Introduction

DNA topoisomerases are important cellular enzymes found in almost all types of living cells. These enzymes mediated the topological adjustments required for DNA replication, transcription, recombination, repair, and chromatin assembly¹⁻³. These enzymes are important molecular drug targets and inhibitors of these enzymes are widely used as effective anticancer agents. Topoisomerase inhibitors are used in clinical treatment of cancer for more than 30 years. About 50% of chemotherapeutic regimens use at least one drug that targets these enzymes⁴. There are two types of topoisomerases in human: type I topoisomerase (Topo I) and type II topoisomerase (Topo II). Topo II has been reported as the specific target of certain most active anticancer drugs such as etoposide, doxorubicin and amscrine⁵. However, Topo II inhibitors have some therapeutic limitations because of their serious side effects during cancer chemotherapy. Thus, development of novel anticancer Topo II inhibitors is necessary for improving cancer treatment⁶⁻¹⁰.

Benzimidazole is found in many clinically useful drugs¹¹ and represents a precious scaffold in the preparation of a wide variety of biological active compounds such as antibacterial, anti-inflammatory and anticancer agents¹². Several benzimidazole derivatives were reported as novel Topo II inhibitors (**1** and **2**, Fig.1). Structure-activity relationship (SAR) studies showed that the benzimidazole rings as a fused system in the structures is significant for Topo II inhibition potency and the phenyl group linked to benzimidazole is particularly important^{13,14}. Mechanism studies and molecular docking revealed that these compounds function as Topo II catalytic inhibitors by blocking the ATP-binding site of the enzyme^{15,16}.

Rhodanine is recognized as a privileged heterocycle in medicinal chemistry¹⁷. The

molecules containing rhodanine moiety are known for their rich pharmacological profile, including antibacterial, anti-parasitic, anti-microbial, anti-tubercular and anticancer¹⁸⁻²¹. Rhodanines possess good activity against different types of cancer including relatively simple derivatives as well as complex or hybrids/conjugates bearing non-fused rhodanine core²²⁻²⁴. For example, commercial GSK1059615 (**3**, Fig. 1) is a reversible, ATP-competitive, inhibitor of PI3K α , which shows potential anticancer activity. Compound **4** (Fig. 1) displays a potent cytotoxicity toward several cancer cell lines.

Pharmacophore hybridization strategy is often used for the design of new drugs and a certain number successful examples are reported in drug discovery and development²⁵⁻²⁸. We have recently designed and synthesized various Topo II inhibitors through pharmacophore hybridization strategy and the results demonstrated that these conjugates possessed generally higher cytotoxicity and Topo II inhibition potency than the individual agents alone^{16,20,29}. In an effort to discover novel anticancer agents that target Topo II more efficiently, benzimidazole-rhodanine conjugates (Fig.1) were synthesized in this work and the Topo I and II inhibition, the DNA interaction, and the cytotoxicity properties of these newly synthesized compounds were evaluated. It was found that these compounds displayed significantly Topo II inhibition potency and showed effective cytotoxicity against six human cancer cell lines.

2. Results and Discussion

2.1. Chemistry

A series of benzimidazole-rhodanine conjugates (**8a-8o**, **9a-9d**, **10a-10h** and **11a-11h**) were synthesized as outlined in Scheme 1. The synthetic strategy consisted of the benzimidazole and rhodanine moieties and then the condensation of them to provide the target

compounds (Fig. 2). Substituted-(benzo[*d*]-imidazole-2-yl)methanols (**1a-1d**) were prepared by refluxing substituted-1,2-diaminobenzene with glycolic acid in hydrochloric acid. Substituted-(1-alkyl-1*H*-benzo[*d*]imidazole-2-yl)methanols (**2a-2s**, **3a-3f** and **4a-4f**) were achieved by *N*-alkylation of **1a-1d** with appropriate benzyl bromide, bromoethane or 2-bromo-1-phenylethanone using K₂CO₃ as base in 27%–88% yield. Substituted-1-alkyl-1*H*-benzo[*d*]imidazole-2-carbaldehydes (**5a-5s**, **6a-6f** and **7a-7f**) were obtained by oxidation of the corresponding primary alcohols with Dess-Martin reagent in 36%–68% yield³⁰. The target compounds (**8a-8o**, **9a-9d**, **10a-10h** and **11a-11h**) were synthesized through the Horner-Wadsworth-Emmons reaction of rhodanine moiety with the prepared aldehydes (**5a-5s**, **6a-6f** and **7a-7f**) in 69%–91% yield. Since the reaction was not region-selective in the preparation of **3a-3f** and **4a-4f**, the R₁ group could be either in C5 or C6 position of benzimidazole scaffold in the process of substitution reaction³¹. 2D NOESY spectrum was performed to determine the isomer of **3a** and **3b** (Fig. S1 and S2). The synthesized compounds were characterized by ¹H NMR, ¹³C NMR, and HRMS (ESI), which was in full accordance with their depicted structures and the purities were confirmed by analytical HPLC.

2.2. Cytotoxicity

The synthesized compounds were evaluated for their cytotoxic activities using the MTT assay against six human cancer cell lines including: the human acute leukemia cell line (HL-60), human cervical cancer cell line (Hela), human breast cancer cell line (MDA-MB-201), adenocarcinomic human alveolar basal epithelial cancer cell line (A549), human lymphoma cancer cell line (Raji), and human prostate cancer cells line (PC-3).

Etoposide and camptothecin were chosen as positive controls. The inhibitory activities (IC_{50}) of the tested compounds are listed in Table 1.

Most of the compounds displayed significant cytotoxic activities with low micromolar IC_{50} values. In addition, a good correlation was found between the Topo II inhibition potency and the cytotoxic activities. Compounds **8g**, **8j**, **8n**, **9a**, **9c**, **10a**, and **10c-10e**, which showed strong Topo II inhibition potency, displayed promising cytotoxic activity against six cancer cell lines. Specially, **8g** and **8j**, which exhibited excellent Topo II inhibition activity at 10 μ M, showed more potent cytotoxic activity, with an IC_{50} values ranging from 0.54 to 3.22 μ M and from 0.21 to 2.67 μ M, respectively. Whereas, others compounds, revealed to be poor Topo II inhibitors showed low or moderate cytotoxic activities. It is worth to mention that HL-60 was revealed more sensitive to these compounds, as a lower IC_{50} value was obtained compared to other cancer cell lines (Table 1).

2.3. Topo II inhibition and SAR study

Topo II-mediated DNA relaxation, cleavage of the complex and unwinding assays as well as molecule docking were performed to evaluate the ability of the synthesized compounds to inhibit Topo II and to investigate their mode of action.

Topo II-mediated DNA relaxation assay was first employed to determine the capacity of these compounds, using etoposide as positive control and pBR322 DNA plasmid as substrate⁸. Compounds **8a-8o** and **9a-9d** (Fig. 2) were first synthesized and submitted to this assay. As shown in Fig. 3A and 3B, most of the tested compounds exhibited significantly Topo II inhibition potency at 50 μ M and displayed a similar effect with etoposide. Compounds **8g**, **8j**, **8n**, **9a**, and **9c** showed the best inhibition potency at 10 μ M (Fig. 3D). It was found that the benzyl group is necessary for the activity (**8f**, Fig. 3A), since its replacement with ethyl group

(**8o**, Fig. 3A) led to a decrease of inhibitory activity. Moreover, compounds **8g** and **8n** with electron donor groups showed better Topo II inhibition than those with electron withdrawing groups (**8a**, **8d**, **8e**, and **8h**, Fig. 3A, 3B and 3D). Along with this observation, **8b**, **8k**, and **8m** with two withdrawing substitution groups on benzyl showed weaker activity than those with one withdrawing substitutions group (**8j**, Fig. 3A, 3B and 3D). The results indicated that benzyl group and the electronic effects of substitutions have significant impact on Topo II inhibitory activity and should be maintained in further structure modification.

In order to investigate the effect of the rhodanine-3-acetic acid moiety on the inhibition of Topo II activity, it was changed to rhodanine (**10g** and **11g**) or rhodanine-3-(3-propionic acid) (**10h** and **11h**). It was found that, the acetic acid moiety was crucial, since **10g**, **11g**, **10h**, and **11h** did not show better Topo II inhibition at 20 μM (Fig. 3C). These results revealed that the acetic acid group linked to rhodanine was also optimal for the activity.

Next, the benzimidazole scaffold was modified with various substitutions ($-\text{F}$, $-\text{Cl}$, and $-\text{OCH}_3$) on the benzene ring. 5 or 6-Monosubstituted isomers can be obtained (**10a-10f** and **11a-11f**, Scheme 2) and no obvious difference in Topo II inhibition potency was observed between the isomers at 50 μM (Fig. 3C). The results showed that **10a**, **10c**, **10d**, and **10e** also displayed strong Topo II inhibition activity even at 10 μM (Fig. 3C and 3D). However, modified **8j** with the same substitutions (**11a-11f**) led to a decrease of Topo II inhibition potency (Fig. 3C and 3D).

Topo I-mediated DNA relaxation assay was employed to study whether this class of compounds also targeted Topo I. The results are presented in Fig. 4. None of the tested compounds exhibited Topo I inhibition potency even at 50 μM , indicating that these

compounds displayed selective inhibition against Topo II.

As compounds **8g** and **8j** showed the best Topo II inhibition and cytotoxic activity, they were selected for the further mechanism studies.

2.4. Compounds **8g** and **8j** are non-intercalative Topo II catalytic inhibitors

Topo II inhibitors have different mechanism of actions. Topo II poisons stabilize the cleavage complex of DNA and promote the formation of linear DNA, whereas Topo II catalytic inhibitors block the activity of the enzyme to perform catalysis¹⁻³. In addition, Topo II catalytic inhibitors can antagonize Topo II poison-mediated DNA damage¹⁶. Topo II-mediated DNA cleavage assay was employed for investigating the mode of action of **8g** and **8j**. As shown in Fig. 5A, etoposide, a classical Topo II poison, produced the linear DNA, while the linear form of the DNA was not observed when **8g** and **8j** were used up to 50 μ M. In addition, pretreatment with **8g** and **8j** could reduce the amount of linear DNA trapped by etoposide. These results provide evidence that **8g** and **8j** act as Topo II catalytic inhibitors.

There are two types of Topo II catalytic inhibitors: DNA intercalators and non-intercalators⁵. Topo I-mediated DNA unwinding assay was carried out to determine whether **8g** and **8j** function as intercalators. In this assay, the supercoiled DNA, relaxed by excessive Topo I, could be regenerated if the test compound is a DNA intercalator. As shown in Fig. 5B, ethidium bromide (EB), a classic intercalator of DNA did help the regeneration of the supercoiled DNA at 5 μ M, while **8g** and **8j** didn't even at 50 μ M. These findings suggest that **8g** and **8j** are non-intercalating Topo II catalytic inhibitors.

2.5. Molecular docking

Molecular docking was carried out to identify the potential interactions of these

compounds with Topo II by using the Surflex-dock program incorporated with the SYBYL software package (Tripos. Inc. St. Louis. MO)^{32,33}. We first docked **8g** and **8j** into various binding pockets in Topo II. The best result was obtained when the compounds were docked into the ATP-binding pocket (PDB code: 1ZXM). As shown in Fig. 6, for both compounds, the nitrogen group (N^3) of benzimidazole formed a special hydrogen bond with the amino group of the residues Asn91, and the carboxylic group formed a hydrogen bond with the amino groups of Arg98 and Asn95. These hydrogen bonds may provide stability to the enzyme-ligand interactions. The benzimidazole group showed hydrophobic interactions with the hydrophobic part of the enzyme, whereas the phenyl group formed hydrophobic interactions with residues Asn150 and Thr159. These results showed that **8g** and **8j** are catalytic inhibitors, whose mode of action seems to occupy the ATP-binding pocket of the ATPase domain of Topo II and make favorable interactions with its key residues.

3. Conclusion

In this study, a series of benzimidazole-rhodanine conjugates were designed and synthesized as potential Topo II-targeting anticancer agents. The results revealed that these compounds displayed strong Topo II inhibition potency and nine of them, namely, **8g**, **8j**, **8n**, **9a**, **9c**, **10a**, **10c**, **10d**, and **10e** almost completely suppressed the Topo II activity at 10 μ M. The SAR study revealed that the benzyl group and the electronic effects of substitutions as well as the rhodanine moiety have significant impact on Topo II inhibition potency. Mechanism studies demonstrated that the leading compounds **8g** and **8j** function as nonintercalative Topo II catalytic inhibitors. The molecular docking analysis suggested that the inhibition mode of **8g** and **8j** may be through blocking the ATP-binding site of the enzyme.

These compounds displayed potent cytotoxic activities with low micromolar IC₅₀ values toward six cancer cell lines. Meanwhile, most of the compounds showed good relationship between their Topo II inhibition potency and the cytotoxicity. In conclusion, the pharmacophore hybridization strategy used in this work on the basis of benzimidazole with rhodanine moiety represents a feasible way to discover Topo II-targeting anticancer agents. Further work is ongoing to optimize the bioactivity of these compounds.

4. Experimental section

4.1. Chemistry

All reagents were commercially available and purchased from Sigma-Aldrich, TCI, AlfaAesar, and Aladdin. They were used without further purification. HPLC grade methanol was order from Sinopharm (China) and silica gel (200-300 mesh, Qingdao Haiyang Chemical Co., Ltd). ¹H and ¹³C NMR spectrum were recorded in DMSO-*d*₆ or CDCl₃ with a Bruker BioSpin GmbH spectrometer at 400 and 101 MHz, respectively. The chemical shifts are reported in parts per million (ppm) relative to residual CDCl₃ ($\delta = 7.26$, ¹H; $\delta = 77.0$, ¹³C) and DMSO-*d*₆ ($\delta = 2.50$, ¹H; $\delta = 39.5$, ¹³C) in the corresponding deuterium agents. High-resolution mass spectra (HRMS) were recorded on Shimadzu LCMS-IT-TO. The melting point (mp) was determined using an SRS-OptiMelt automated melting point instrument without correction. The purities of synthesized compounds were confirmed by analytical HPLC performed with a dual pump Shimadzu LC-20AB system equipped with an Ultimate XB-C18 column and eluted with methanol/water (80%) at a flow rate of 0.5 mL·min⁻¹, and the purities were proved to be higher than 95%. The chemical structure and the general method for the synthesis of the intermediates are list in Supporting Information.

4.2. General method for synthesis of the target compounds (8a–8o, 9a–9d, 10a–10h and

11a–11h).

A mixture of the appropriate aldehydes (**5a–5s**, **6a–6f** and **7a–7f**, 0.1 mmol), the rhodanine moiety (0.1 mmol), and NaOAc (0.3 mmol) in acetic acid (6 mL) heated to 110 °C for 4 h. Then, it was cooled to room temperature and poured into water. The product was then filtered through the suction pump, washed with water/EtOH (1/1, v/v) to remove the excess acetic acid and recrystallized from EtOH.

4.2.1. (Z)-2-(5-((1-(4-bromobenzyl)-1H-benzo[d]imidazol-2-yl)methylene)-4-oxo-2-thioxothiazolidin-3-yl)acetic acid (8a). Rhodanine-3-acetic acid and **5a** were used as reactants to give **8a**. Yellow solid, yield: 73%, mp: 297.1–299.2 °C. ¹H NMR (400 MHz, DMSO-*d*₆) δ 13.45 (s, 1H), 7.97 (s, 1H), 7.85 (d, *J* = 7.5 Hz, 1H), 7.69 (d, *J* = 7.7 Hz, 1H), 7.53 (d, *J* = 8.1 Hz, 2H), 7.41 – 7.33 (m, 2H), 7.10 (d, *J* = 8.0 Hz, 2H), 5.88 (s, 2H), 4.74 (s, 2H). ¹³C NMR (101 MHz, DMSO-*d*₆) δ 198.3, 167.8, 166.3, 147.8, 143.6, 136.9, 135.9, 132.3, 130.3, 129.2, 125.5, 124.3, 121.4, 120.6, 116.4, 112.0, 46.1, 45.2. HRMS (ESI): C₂₀H₁₄BrN₃O₃S₂ [M + H]⁺487.9717, found 487.9711.

4.2.2. (Z)-2-(5-((1-(4-bromo-2-fluorobenzyl)-1H-benzo[d]imidazol-2-yl)methylene)-4-oxo-2-thioxothiazolidin-3-yl)acetic acid (8b). Rhodanine-3-acetic acid and **5b** were used as reactants to give **8b**. Yellow solid, yield: 86%, mp: 283.7–285.4 °C. ¹H NMR (400 MHz, DMSO-*d*₆) δ 13.46 (s, 1H), 8.03 (s, 1H), 7.85 (d, *J* = 7.4 Hz, 1H), 7.67 (d, *J* = 7.6 Hz, 1H), 7.60 (d, *J* = 9.9 Hz, 1H), 7.39 – 7.33 (m, 3H), 7.05 (t, *J* = 8.2 Hz, 1H), 5.91 (s, 2H), 4.75 (s, 2H). ¹³C NMR (101 MHz, DMSO-*d*₆) δ 198.3, 167.8, 166.3 (d, *J* = 251.0 Hz), 161.6, 159.1, 147.9, 143.5, 135.7, 131.1 (d, *J* = 4.5 Hz), 130.2, 128.5 (d, *J* = 3.5 Hz), 125.5, 124.3, 123.7 (d,

$J = 14.7$ Hz), 122.0 (d, $J = 9.6$ Hz), 120.6, 119.6 (d, $J = 24.5$ Hz), 116.6, 111.9, 45.2, 41.4 (d, $J = 2.6$ Hz). HRMS (ESI): calcd for $C_{20}H_{13}BrFN_3O_3S_2$ $[M + H]^+$ 505.9663, found 505.9658.

4.2.3 (Z)-2-(5-((1-(4-cyanobenzyl)-1H-benzof[d]imidazol-2-yl)methylene)-4-oxo-2-thioxothiazolidin-3-yl) acetic acid (8c). Rhodanine-3-acetic acid and **5c** were used as reactants to give **8c**. Yellow solid, yield: 91%, mp: 284.6–286.3 °C. 1H NMR (400 MHz, DMSO- d_6) δ 13.47 (s, 1H), 7.96 (s, 1H), 7.87 (d, $J = 7.0$ Hz, 1H), 7.81 (d, $J = 8.0$ Hz, 2H), 7.66 (d, $J = 8.0$ Hz, 1H), 7.41 – 7.34 (m, 2H), 7.28 (d, $J = 8.0$ Hz, 2H), 6.02 (s, 2H), 4.74 (s, 2H). ^{13}C NMR (101 MHz, DMSO- d_6) δ 198.2, 167.8, 166.3, 147.9, 143.56, 143.0, 135.9, 133.3, 130.5, 127.8, 125.6, 124.4, 120.6, 119.0, 116.2, 111.9, 111.1, 46.3, 45.2. HRMS (ESI): calcd for $C_{20}H_{14}FN_3O_3S_2$ $[M + H]^+$ 435.0531, found 435.0542.

4.2.4. (Z)-2-(5-((1-(4-nitrobenzyl)-1H-benzof[d]imidazol-2-yl)methylene)-4-oxo-2-thioxothiazolidin-3-yl)acetic acid (8d). Rhodanine-3-acetic acid and **5d** were used as reactants to give **8d**. Yellow solid, yield: 79%, mp: 290.5–292.3 °C. 1H NMR (400 MHz, DMSO- d_6) δ 13.44 (s, 1H), 8.20 (d, $J = 8.4$ Hz, 2H), 7.97 (s, 1H), 7.88 (d, $J = 6.5$ Hz, 1H), 7.67 (d, $J = 8.1$ Hz, 1H), 7.41 – 7.33 (m, 4H), 6.08 (s, 2H), 4.74 (s, 2H). ^{13}C NMR (101 MHz, DMSO- d_6) δ 198.2, 167.7, 166.2, 147.8, 147.5, 144.9, 143.6, 135.8, 130.5, 128.1, 125.6, 124.5, 124.4, 120.7, 116.2, 111.9, 46.2, 45.2. HRMS (ESI): calcd for $C_{20}H_{14}N_4O_5S_2$ $[M + H]^+$ 455.0439, found 455.0427.

4.2.5. (Z)-2-(5-((1-(4-fluorobenzyl)-1H-benzof[d]imidazol-2-yl)methylene)-4-oxo-2-thioxothiazolidin-3-yl)acetic acid (8e). Rhodanine-3-acetic acid and **5e** were used as reactants to give **8e**. Yellow solid, yield: 83%, mp: 287.7–289.2 °C. 1H NMR (400 MHz, DMSO- d_6) δ 13.46 (s, 1H), 7.99 (s, 1H), 7.85 (d, $J = 7.6$ Hz, 1H), 7.72 (d, $J = 7.9$ Hz, 1H), 7.41 – 7.33 (m,

2H), 7.23 – 7.15 (m, 4H), 5.88 (s, 2H), 4.74 (s, 2H). ^{13}C NMR (101 MHz, DMSO- d_6) δ 198.3, 167.8, 166.3, 162.1(d, $J = 244.0$ Hz), 147.7, 143.6, 135.9, 133.6 (d, $J = 3.0$ Hz), 130.3, 129.2 (d, $J = 8.4$ Hz), 125.5, 124.3, 120.6, 116.4, 116.1 (d, $J = 21.6$ Hz), 112.0, 46.0, 45.2. HRMS (ESI): calcd for $\text{C}_{21}\text{H}_{14}\text{N}_4\text{O}_3\text{S}_2$ $[\text{M} + \text{H}]^+$ 428.0508, found 428.0524.

4.2.6. *(Z)-2-(5-((1-benzyl-1H-benzo[d]imidazol-2-yl)methylene)-4-oxo-2-thioxothiazolidin-3-yl)acetic acid (8f)*. Rhodanine-3-acetic acid and **5f** were used as reactants to give **8f**. Yellow solid, yield: 77%, mp: 293.4–295.1 °C. ^1H NMR (400 MHz, DMSO- d_6) δ 13.45 (s, 1H), 7.97 (s, 1H), 7.85 (d, $J = 7.4$ Hz, 1H), 7.72 (d, $J = 8.0$ Hz, 1H), 7.40 – 7.32 (m, 4H), 7.29 – 7.24 (m, 1H), 7.15 (d, $J = 7.5$ Hz, 2H), 5.89 (s, 2H), 4.74 (s, 2H). ^{13}C NMR (101 MHz, DMSO- d_6) δ 198.3, 167.8, 166.3, 147.8, 143.6, 137.4, 136.0, 130.1, 129.4, 128.2, 127.0, 125.4, 124.2, 120.6, 116.5, 112.0, 46.7, 45.2. HRMS (ESI): calcd for $\text{C}_{20}\text{H}_{15}\text{N}_3\text{O}_3\text{S}_2$ $[\text{M} + \text{H}]^+$ 409.0619, found 409.0627.

4.2.7. *(Z)-2-(5-((1-(4-methylbenzyl)-1H-benzo[d]imidazol-2-yl)methylene)-4-oxo-2-thioxothiazolidin-3-yl)acetic acid (8g)*. Rhodanine-3-acetic acid and **5g** were used as reactants to give **8g**. Yellow solid, yield: 87%, mp: >300 °C. ^1H NMR (400 MHz, DMSO- d_6) δ 13.47 (s, 1H), 7.95 (s, 1H), 7.84 (d, $J = 7.6$ Hz, 1H), 7.72 (d, $J = 7.8$ Hz, 1H), 7.40 – 7.32 (m, 2H), 7.16 – 7.10 (m, 2H), 7.08 – 7.02 (m, 2H), 5.82 (s, 2H), 4.74 (s, 2H), 2.23 (s, 3H). ^{13}C NMR (101 MHz, DMSO- d_6) δ 198.3, 167.8, 166.3, 147.7, 143.6, 137.6, 136.0, 134.4, 130.1, 129.9, 127.0, 125.4, 124.2, 120.5, 116.6, 112.1, 46.5, 45.3, 21.1. HRMS (ESI): calcd for $\text{C}_{21}\text{H}_{17}\text{N}_3\text{O}_3\text{S}_2$ $[\text{M} + \text{H}]^+$ 424.0753, found 424.0739.

4.2.8. *(Z)-2-(5-((1-(4-chlorobenzyl)-1H-benzo[d]imidazol-2-yl)methylene)-4-oxo-2-thioxothiazolidin-3-yl)acetic acid (8h)*. Rhodanine-3-acetic acid and **5h** were used as

reactants to give **8h**. Yellow solid, yield: 90%, mp: >300 °C. ¹H NMR (400 MHz, DMSO-*d*₆) δ 13.46 (s, 1H), 7.97 (s, 1H), 7.85 (d, *J* = 7.6 Hz, 1H), 7.70 (d, *J* = 7.7 Hz, 1H), 7.42 – 7.33 (m, 4H), 7.19 – 7.15 (m, 2H), 5.89 (s, 2H), 4.74 (s, 2H). ¹³C NMR (101 MHz, DMSO-*d*₆) δ 198.3, 167.8, 166.3, 147.8, 143.6, 136.5, 135.9, 132.9, 130.3, 129.4, 128.9, 125.5, 124.3, 120.6, 116.4, 112.0, 46.0, 45.2. HRMS (ESI): calcd for C₂₀H₁₄ClN₃O₃S₂ [M + H]⁺ 444.0212, found 444.0226.

4.2.9. *(Z)*-2-(5-((1-(4-trifluoromethylbenzyl)-1H-benzo[d]imidazol-2-yl)methylene)-4-oxo-2-thioxo thiazolidin-3-yl)acetic acid (**8i**). Rhodanine-3-acetic acid and **5i** were used as reactants to give **8i**. Yellow solid, yield: 81%, mp: 281.8–283.4 °C. ¹H NMR (400 MHz, DMSO-*d*₆) δ 13.44 (s, 1H), 7.98 (s, 1H), 7.87 (d, *J* = 7.1 Hz, 1H), 7.70 (m, 3H), 7.42 – 7.35 (m, 2H), 7.32 (d, *J* = 8.0 Hz, 2H), 6.02 (s, 2H), 4.74 (s, 2H). ¹³C NMR (101 MHz, DMSO-*d*₆) δ 198.3, 167.7, 166.3, 147.9, 143.6, 142.1, 135.9, 130.5, 128.8 (q, *J* = 32.0 Hz), 127.7, 126.3, (q, *J* = 3.7 Hz), 125.6, 124.6 (q, *J* = 272.0 Hz), 120.6, 116.3, 111.2, 46.2, 45.2. HRMS (ESI): calcd for C₂₁H₁₄F₃N₃O₃S₂ [M + H]⁺ 478.0471, found 478.0462.

4.2.10. *(Z)*-2-(5-((1-(2-fluorobenzyl)-1H-benzo[d]imidazol-2-yl)methylene)-4-oxo-2-thioxothiazolidin-3-yl)acetic acid (**8j**). Rhodanine-3-acetic acid and **5j** were used as reactants to give **8j**. Yellow solid, yield: 82%, mp: 272.6–274.2 °C. ¹H NMR (400 MHz, DMSO-*d*₆) δ 13.44 (s, 1H), 8.03 (s, 1H), 7.84 (d, *J* = 7.2 Hz, 1H), 7.69 (d, *J* = 7.3 Hz, 1H), 7.42 – 7.31 (m, 3H), 7.29 – 7.20 (m, 1H), 7.19 – 7.07 (m, 2H), 5.93 (s, 2H), 4.75 (s, 2H). ¹³C NMR (101 MHz, DMSO-*d*₆) δ 198.4, 167.8, 166.3, 160.5 (d, *J* = 245.7 Hz), 147.9, 143.5, 135.8, 130.7 (d, *J* = 8.2 Hz), 130.1, 129.6 (d, *J* = 3.8 Hz), 125.4 (d, *J* = 2.3 Hz), 125.4, 124.2,

124.0(d, $J = 14.5$ Hz), 120.6, 116.7, 116.2 (d, $J = 20.9$ Hz), 112.0, 45.2, 41.7 (d, $J = 3.4$ Hz).

HRMS (ESI): calcd for $C_{20}H_{14}FN_3O_3S_2$ $[M + H]^+$ 428.0516, found 428.0523.

4.2.11. *(Z)-2-(5-((1-(2,4-difluorobenzyl)-1H-benzo[d]imidazol-2-yl)methylene)-4-oxo-2-thioxothiazolidin-3-yl)acetic acid (8k)*. Rhodanine-3-acetic acid and **5k** were used as reactants to give **8k**. Yellow solid, yield: 77%, mp: 261.8–263.3 °C. 1H NMR (400 MHz, DMSO- d_6) δ 13.48 (s, 1H), 8.05 (s, 1H), 7.84 (d, $J = 7.6$ Hz, 1H), 7.69 (d, $J = 7.7$ Hz, 1H), 7.44 – 7.19 (m, 4H), 7.06 (t, $J = 8.5$ Hz, 1H), 5.90 (s, 2H), 4.75 (s, 2H). ^{13}C NMR (101 MHz, DMSO- d_6) δ 198.4, 167.8, 166.3, 162.5 (dd, $J = 247.2, 12.2$ Hz), 160.64 (dd, $J = 248.9, 12.5$ Hz), 147.8, 143.5, 135.7, 131.1 (dd, $J = 10.0, 5.5$ Hz), 130.1, 125.4, 124.3, 120.6, 120.5 (dd, $J = 14.8, 3.6$ Hz), 116.6, 112.4 (dd, $J = 21.3, 3.5$ Hz), 111.95, 104.9 (t, $J = 25.8$ Hz), 45.2, 41.3 (d, $J = 2.4$ Hz). HRMS (ESI): calcd for $C_{20}H_{13}F_2N_3O_3S_2$ $[M + H]^+$ 446.0427, found 446.0438.

4.2.12. *(Z)-2-(5-((1-(3-fluorobenzyl)-1H-benzo[d]imidazol-2-yl)methylene)-4-oxo-2-thioxothiazolidin-3-yl)acetic acid (8l)*. Rhodanine-3-acetic acid and **5l** were used as reactants to give **8l**. Yellow solid, yield: 71%, mp: 288.2–290.6 °C. 1H NMR (400 MHz, DMSO- d_6) δ 13.55 (s, 1H), 7.97 (s, 1H), 7.86 (d, $J = 7.4$ Hz, 1H), 7.71 (d, $J = 7.7$ Hz, 1H), 7.45 – 7.32 (m, 3H), 7.12 (t, $J = 8.5$ Hz, 1H), 7.05 (d, $J = 9.8$ Hz, 1H), 6.90 (d, $J = 7.6$ Hz, 1H), 5.91 (s, 2H), 4.74 (s, 2H). ^{13}C NMR (101 MHz, DMSO- d_6) δ 198.3, 167.8, 166.3, 162.7 (d, $J = 244.7$ Hz), 147.8, 143.6, 140.2 (d, $J = 7.2$ Hz), 135.9, 131.5 (d, $J = 8.4$ Hz), 130.4, 125.56, 124.3, 122.9 (d, $J = 2.6$ Hz), 120.6, 116.3, 115.1 (d, $J = 20.9$ Hz), 114.0 (d, $J = 22.1$ Hz), 111.9, 46.2 (d, $J = 0.6$ Hz), 45.2. HRMS (ESI): calcd for $C_{20}H_{14}FN_3O_3S_2$ $[M + H]^+$ 428.0516, found 428.0522.

4.2.13. *(Z)-2-(5-((1-(3,4-difluorobenzyl)-1H-benzo[d]imidazol-2-yl)methylene)-4-oxo-2-thioxothiazolidin-3-yl)acetic acid (8m)*. Rhodanine-3-acetic acid and **5m** were used as

reactants to give **8m**. Yellow solid, yield: 76%, mp: 267.6–269.2 °C. ¹H NMR (400 MHz, DMSO-*d*₆) δ 13.46 (s, 1H), 8.00 (s, 1H), 7.85 (d, *J* = 7.6 Hz, 1H), 7.70 (d, *J* = 7.8 Hz, 1H), 7.48 – 7.28 (m, 4H), 6.93 (s, 1H), 5.88 (s, 2H), 4.75 (s, 2H). ¹³C NMR (101 MHz, DMSO-*d*₆) δ 198.3, 167.8, 166.3, 149.9 (dd, *J* = 246.8, 12.8 Hz), 149.4 (dd, *J* = 246.1, 12.4 Hz), 147.8, 143.6, 135.8, 135.1 (dd, *J* = 5.4, 3.9 Hz), 130.4, 125.6, 124.3, 123.9 (dd, *J* = 6.7, 3.5 Hz), 120.6, 118.5 (d, *J* = 17.4 Hz), 116.6 (d, *J* = 17.8 Hz), 116.3, 111.9, 45.7, 45.2. HRMS (ESI): calcd for C₂₀H₁₃F₂N₃O₃S₂ [M + H]⁺ 446.0527, found 446.0532.

4.2.14. *(Z)-2-(5-((1-(3,5-dimethoxybenzyl)-1H-benzof[d]imidazol-2-yl)methylene)-4-oxo-2-thioxothiazolidin-3-yl)acetic acid (8n)*. Rhodanine-3-acetic acid and **5n** were used as reactants to give **8n**. Yellow solid, yield: 78%, mp: 259.8–261.3 °C. ¹H NMR (400 MHz, DMSO-*d*₆) δ 7.95 (s, 1H), 7.85 (d, *J* = 7.5 Hz, 1H), 7.74 (d, *J* = 8.0 Hz, 1H), 7.44 – 7.33 (m, 2H), 6.41 (t, *J* = 2.1 Hz, 1H), 6.27 (d, *J* = 2.1 Hz, 2H), 5.79 (s, 2H), 4.74 (s, 2H), 3.66 (s, 6H). ¹³C NMR (101 MHz, DMSO-*d*₆) δ 198.3, 167.7, 166.3, 161.3, 147.8, 143.5, 139.7, 136.1, 130.1, 125.5, 124.2, 120.6, 116.5, 112.0, 105.4, 99.3, 55.7, 46.6, 45.2. HRMS (ESI): calcd for C₂₂H₁₉N₃O₅S₂[M + H]⁺ 470.0882, found 470.0871.

4.2.15. *(Z)-2-(5-((1-ethyl-1H-benzof[d]imidazol-2-yl)methylene)-4-oxo-2-thioxothiazolidin-3-yl)acetic acid (8o)*. Rhodanine-3-acetic acid and **5o** were used as reactants to give **8o**. Yellow solid, yield: 81%, mp: 226.5–227.8 °C. ¹H NMR (400 MHz, DMSO-*d*₆) δ 13.45 (s, 1H), 7.93 (s, 1H), 7.81 (d, *J* = 8.0 Hz, 1H), 7.73 (d, *J* = 8.1 Hz, 1H), 7.40 (t, *J* = 7.2 Hz, 1H), 7.34 (t, *J* = 7.2 Hz, 1H), 4.76 (s, 2H), 4.60 (q, *J* = 7.1 Hz, 2H), 1.36 (t, *J* = 7.1 Hz, 3H). ¹³C NMR (101 MHz, DMSO-*d*₆) δ 198.4, 167.8, 166.4, 147.0, 143.6, 135.4,

129.7, 125.2, 124.0, 120.5, 116.6, 111.7, 45.2, 38.7, 16.3. HRMS (ESI): calcd for $C_{15}H_{13}N_3O_3S_2$ $[M + H]^+$ 348.0428, found 348.0422.

4.2.16. (Z)-2-(5-((1-(2-(4-fluorophenyl)-2-oxoethyl)-1H-benzof[d]imidazol-2-yl)methylene)-4-oxo-2-thioxothiazolidin-3-yl)acetic acid (9a). Rhodanine-3-acetic acid and **5p** were used as reactants to give **9a**. Yellow solid, yield: 81%, mp: 247.7–249.3 °C. 1H NMR (400 MHz, DMSO- d_6) δ 8.27 – 8.21 (m, 2H), 7.97 (s, 1H), 7.89 – 7.85 (m, 1H), 7.68 – 7.64 (m, 1H), 7.51 (t, J = 8.7 Hz, 2H), 7.38 – 7.32 (m, 2H), 6.42 (s, 2H), 4.75 (s, 2H). ^{13}C NMR (101 MHz, DMSO) δ 198.5, 192.3, 167.8, 166.3, 166.1(d, J = 253.2 Hz), 148.8, 143.4, 136.5, 132.1 (d, J = 9.7 Hz), 131.6 (d, J = 2.7 Hz), 129.8, 125.2, 124.1, 120.4, 117.4, 116.4 (d, J = 22.1 Hz), 111.89, 50.6, 45.2. HRMS (ESI): calcd for $C_{21}H_{14}FN_3O_4S_2$ $[M + H]^+$ 456.0429, found 456.0431.

4.2.17. (Z)-2-(5-((1-(2-(4-methoxyphenyl)-2-oxoethyl)-1H-benzof[d]imidazol-2-yl)methylene)-4-oxo-2-thioxothiazolidin-3-yl)acetic acid (9b). Rhodanine-3-acetic acid and **5q** were used as reactants to give **9b**. Yellow solid, yield: 72%, mp: 256.4–258.1 °C. δ 13.36 (s, 1H), 8.12 (d, J = 8.7 Hz, 2H), 7.90 (s, 1H), 7.88 – 7.82 (m, 1H), 7.67 – 7.61 (m, 1H), 7.38 – 7.32 (m, 2H), 7.17 (d, J = 8.7 Hz, 2H), 6.37 (s, 2H), 4.74 (s, 2H), 3.90 (s, 3H). ^{13}C NMR (101 MHz, DMSO- d_6) δ 198.5, 191.8, 167.8, 166.3, 164.5, 148.8, 143.5, 136.5, 131.4, 129.7, 127.7, 125.2, 124.0, 120.4, 117.4, 114.6, 111.8, 56.2, 50.2, 45.2. HRMS (ESI): calcd for $C_{22}H_{17}N_3O_5S_2$ $[M + H]^+$ 468.0653, found 468.0641.

4.2.18. (Z)-2-(5-((1-(2-(4-chlorophenyl)-2-oxoethyl)-1H-benzof[d]imidazol-2-yl)methylene)-4-oxo-2-thioxothiazolidin-3-yl)acetic acid (9c). Rhodanine-3-acetic acid and **5r** were used as reactants to give **9c**. Yellow solid, yield: 83%, mp: 256.9–258.2 °C. 1H NMR (400 MHz,

DMSO- d_6) δ 8.16 (d, $J = 8.5$ Hz, 2H), 7.98 (s, 1H), 7.90 – 7.83 (m, 1H), 7.76 (d, $J = 8.5$ Hz, 2H), 7.69 – 7.63 (m, 1H), 7.38 – 7.32 (m, 2H), 6.44 (d, $J = 19.5$ Hz, 2H), 4.74 (s, 2H). ^{13}C NMR (101 MHz, DMSO- d_6) δ 198.5, 192.7, 167.8, 166.3, 148.8, 143.4, 139.6, 136.5, 133.5, 130.9, 129.8, 129.4, 125.2, 124.1, 120.4, 117.4, 111.9, 50.6, 45.2. HRMS (ESI): calcd for $\text{C}_{22}\text{H}_{17}\text{ClN}_3\text{O}_4\text{S}_2$ $[\text{M} + \text{H}]^+$ 472.0193, found 472.0172.

4.2.19. *(Z)-2-(4-oxo-5-((1-(2-oxo-2-(p-tolyl)ethyl)-1H-benzo[d]imidazol-2-yl)methylene)-2-thioxothiazolidin-3-yl)acetic acid (9d)*. Rhodanine-3-acetic acid and **5s** were used as reactants to give **9d**. Yellow solid, yield: 76%, mp: 263.1–265.3 °C. ^1H NMR (400 MHz, DMSO- d_6) δ 8.06 (d, $J = 7.7$ Hz, 2H), 7.93 (s, 1H), 7.88 – 7.84 (m, 1H), 7.67 – 7.63 (m, 1H), 7.47 (d, $J = 7.6$ Hz, 2H), 7.40 – 7.34 (s, 2H), 6.39 (s, 2H), 4.74 (s, 2H), 2.46 (s, 3H). ^{13}C NMR (101 MHz, DMSO- d_6) δ 198.5, 193.1, 167.8, 166.3, 148.8, 145.3, 143.5, 136.5, 132.3, 129.9, 129.7, 129.1, 125.2, 124.1, 120.4, 117.4, 111.8, 50.4, 45.2, 21.8. HRMS (ESI): calcd for $\text{C}_{22}\text{H}_{17}\text{N}_3\text{O}_4\text{S}_2$ $[\text{M} + \text{H}]^+$ 452.0727, found 452.0731.

4.2.20. *(Z)-2-(5-((5-chloro-1-(4-methylbenzyl)-1H-benzo[d]imidazol-2-yl)methylene)-4-oxo-2-thioxothiazolidin-3-yl)acetic acid (10a)*. Rhodanine-3-acetic acid and **6a** were used as reactants to give **10a**. Yellow solid, yield: 84%, mp: 297.9–299.3 °C. ^1H NMR (400 MHz, DMSO- d_6) δ 13.48 (s, 1H), 7.95 – 7.91 (m, 2H), 7.77 (d, $J = 8.8$ Hz, 1H), 7.42 (dd, $J = 8.7$, 1.8 Hz, 1H), 7.14 (d, $J = 8.0$ Hz, 2H), 7.05 (d, $J = 8.0$ Hz, 2H), 5.83 (s, 2H), 4.74 (s, 2H), 2.24 (s, 3H). ^{13}C NMR (101 MHz, DMSO- d_6) δ 198.0, 167.8, 166.3, 148.8, 142.2, 137.6, 136.7, 134.2, 130.8, 123.0, 129.9, 127.0, 124.7, 121.9, 116.1, 111.9, 46.6, 45.3, 21.1. HRMS (ESI): calcd for $\text{C}_{21}\text{H}_{16}\text{ClN}_3\text{O}_3\text{S}_2$ $[\text{M} + \text{H}]^+$ 458.0334, found 458.0329.

4.2.21. *(Z)-2-(5-((6-chloro-1-(4-methylbenzyl)-1H-benzod[imidazol-2-yl)methylene]-4-oxo-2-thioxothiazolidin-3-yl)acetic acid (10b)*. Rhodanine-3-acetic acid and **6b** were used as reactants to give **10b**. Yellow solid, yield: 69%, mp: >300 °C. ¹H NMR (400 MHz, DMSO-*d*₆) δ 13.48 (s, 1H), 7.94 – 7.91 (m, 2H), 7.86 (d, *J* = 8.7 Hz, 1H), 7.37 (dd, *J* = 8.7, 1.9 Hz, 1H), 7.15 (d, *J* = 7.9 Hz, 2H), 7.05 (d, *J* = 8.0 Hz, 2H), 5.83 (s, 2H), 4.74 (s, 2H), 2.25 (s, 3H). ¹³C NMR (101 MHz, DMSO-*d*₆) δ 198.1, 167.8, 166.3, 149.1, 144.1, 137.6, 134.8, 134.2, 131.1, 129.9, 128.7, 127.0, 125.5, 119.8, 116.9, 113.5, 46.7, 45.2, 21.1. HRMS (ESI): calcd for C₂₁H₁₆ClN₃O₃S₂ [M + H]⁺458.0334, found 458.0343.

4.2.22. *(Z)-2-(5-((5-fluoro-1-(4-methylbenzyl)-1H-benzod[imidazol-2-yl)methylene]-4-oxo-2-thioxothiazolidin-3-yl)acetic acid (10c)*. Rhodanine-3-acetic acid and **6c** were used as reactants to give **10c**. Yellow solid, yield: 77%, mp: 291.5–292.9 °C. ¹H NMR (400 MHz, DMSO-*d*₆) δ 13.44 (s, 1H), 7.96 (s, 1H), 7.78 – 7.74 (m, 1H), 7.68 (dd, *J* = 9.5, 2.4 Hz, 1H), 7.32 – 7.24 (m, 1H), 7.15 (d, *J* = 8.0 Hz, 2H), 7.07 (d, *J* = 8.0 Hz, 2H), 5.85 (s, 2H), 4.76 (s, 2H), 2.25 (s, 3H). ¹³C NMR (101 MHz, DMSO-*d*₆) δ 198.1, 167.8, 166.3, 159.9 (d, *J* = 238.1 Hz), 149.1, 143.7 (d, *J* = 13.3 Hz), 137.6, 134.3, 132.8, 130.7, 129.9, 127.0, 116.2, 114.0 (d, *J* = 26.7 Hz), 113.2 (d, *J* = 10.5 Hz), 105.7 (d, *J* = 24.1 Hz), 46.7, 45.3, 21.1. HRMS (ESI): calcd for C₂₁H₁₆FN₃O₃S₂ [M + H]⁺442.0651, found 442.0641.

4.2.23. *(Z)-2-(5-((6-fluoro-1-(4-methylbenzyl)-1H-benzod[imidazol-2-yl)methylene]-4-oxo-2-thioxothiazolidin-3-yl)acetic acid (10d)*. Rhodanine-3-acetic acid and **6d** were used as reactants to give **10d**. Yellow solid, yield: 73%, mp: >300 °C. ¹H NMR (400 MHz, DMSO-*d*₆) δ 13.48 (s, 1H), 7.93 (s, 1H), 7.91 – 7.87 (m, 1H), 7.70 (dd, *J* = 9.2, 2.4 Hz, 1H), 7.27 – 7.21 (m, 1H), 7.16 (d, *J* = 8.0 Hz, 2H), 7.08 (d, *J* = 8.0 Hz, 2H), 5.82 (s, 2H), 4.75 (s,

2H), 2.26 (s, 3H). ^{13}C NMR (101 MHz, DMSO- d_6) δ 198.1, 167.8, 166.38, 160.6 (d, $J = 241.1$ Hz), 148.7 (d, $J = 3.2$ Hz), 140.2, 137.6, 136.5, 134.2, 129.9, 127.1, 127.0, 121.9 (d, $J = 10.4$ Hz), 116.3, 112.9 (d, $J = 26.0$ Hz), 98.5 (d, $J = 27.9$ Hz), 46.6, 45.2, 21.1. HRMS (ESI): calcd for $\text{C}_{21}\text{H}_{16}\text{FN}_3\text{O}_3\text{S}_2$ $[\text{M} + \text{H}]^+$ 442.0651, found 442.0647.

4.2.24. *(Z)-2-(5-((5-methoxy-1-(4-methylbenzyl)-1H-benzo[d]imidazol-2-yl)methylene)-4-oxo-2-thioxothiazolidin-3-yl)acetic acid (10e)*. Rhodanine-3-acetic acid and **6e** were used as reactants to give **10e**. Yellow solid, yield: 85%, mp: 295.3–296.6 °C. ^1H NMR (400 MHz, DMSO- d_6) δ 13.44 (s, 1H), 7.92 (s, 1H), 7.61 (d, $J = 9.0$ Hz, 1H), 7.32 (d, $J = 2.3$ Hz, 1H), 7.13 (d, $J = 8.0$ Hz, 2H), 7.05 – 7.00 (m, 3H), 5.78 (s, 2H), 4.73 (s, 2H), 3.83 (s, 3H), 2.23 (s, 3H). ^{13}C NMR (101 MHz, DMSO- d_6) δ 198.3, 167.8, 166.3, 157.4, 147.5, 144.6, 137.5, 134.5, 130.8, 129.9, 129.1, 127.0, 116.6, 116.5, 112.6, 101.5, 56.1, 46.5, 45.2, 21.1. HRMS (ESI): calcd for $\text{C}_{22}\text{H}_{19}\text{N}_3\text{O}_4\text{S}_2$ $[\text{M} + \text{H}]^+$ 454.0821, found 454.0826.

4.2.25. *(Z)-2-(5-((6-methoxy-1-(4-methylbenzyl)-1H-benzo[d]imidazol-2-yl)methylene)-4-oxo-2-thioxothiazolidin-3-yl)acetic acid (10f)*. Rhodanine-3-acetic acid and **6f** were used as reactants to give **10f**. Yellow solid, yield: 84%, mp: 294.2–295.7 °C. ^1H NMR (400 MHz, DMSO- d_6) δ 13.43 (s, 1H), 7.84 (s, 1H), 7.73 (d, $J = 8.9$ Hz, 1H), 7.29 (d, $J = 2.2$ Hz, 1H), 7.14 (d, $J = 8.0$ Hz, 2H), 7.05 (d, $J = 8.0$ Hz, 2H), 6.98 (dd, $J = 8.9, 2.3$ Hz, 1H), 5.79 (s, 2H), 4.72 (s, 2H), 3.82 (s, 3H), 2.24 (s, 3H). ^{13}C NMR (101 MHz, DMSO- d_6) δ 198.2, 167.8, 166.3, 158.6, 146.8, 138.5, 137.5, 137.2, 134.5, 129.9, 127.8, 127.0, 121.4, 116.7, 115.0, 94.2, 56.3, 46.2, 45.2, 21.1. HRMS (ESI): calcd for $\text{C}_{22}\text{H}_{19}\text{N}_3\text{O}_4\text{S}_2$ $[\text{M} + \text{H}]^+$ 454.0821, found 454.0812.

4.2.26. *(Z)-5-((1-(4-methylbenzyl)-1H-benzo[d]imidazol-2-yl)methylene)-2-thioxothiazolidin-4-one (10g)*. Rhodanine and **5g** were used as reactants to give **10g**. Yellow

solid, yield: 86%, mp: >300 °C. ^1H NMR (400 MHz, DMSO- d_6) δ 13.77 (s, 1H), 7.80 (d, J = 7.5 Hz, 1H), 7.70 (d, J = 6.8 Hz, 2H), 7.38 – 7.30 (m, 2H), 7.12 (d, J = 7.9 Hz, 2H), 7.03 (d, J = 7.9 Hz, 2H), 5.78 (s, 2H), 2.23 (s, 3H). ^{13}C NMR (101 MHz, DMSO- d_6) δ 200.7, 169.2, 147.8, 143.5, 137.5, 136.0, 134.5, 133.8, 129.9, 127.0, 125.1, 124.0, 120.4, 114.5, 111.9, 46.4, 21.1. HRMS (ESI): calcd for $\text{C}_{19}\text{H}_{15}\text{N}_3\text{OS}_2$ $[\text{M} + \text{H}]^+$ 366.0752, found 366.0743.

4.2.27. *(Z)-3-(5-((1-(4-methylbenzyl)-1H-benzo[d]imidazol-2-yl)methylene)-4-oxo-2-thioxothiazolidin-3-yl)propanoic acid (10h)*. Rhodanine-3-propanoic acid and **5g** were used as reactants to give **10h**. Yellow solid, yield: 92%, mp: 267.1–269.6 °C. ^1H NMR (400 MHz, DMSO- d_6) δ 12.49 (s, 1H), 7.86 (s, 1H), 7.82 (d, J = 7.4 Hz, 1H), 7.71 (d, J = 8.0 Hz, 1H), 7.35 (dq, J = 13.5, 6.6 Hz, 2H), 7.13 (d, J = 7.9 Hz, 2H), 7.03 (d, J = 8.0 Hz, 2H), 5.81 (s, 2H), 4.25 – 4.20 (m, 2H), 2.67 – 2.62 (m, 2H), 2.23 (s, 3H). ^{13}C NMR (101 MHz, DMSO- d_6) δ 198.4, 172.2, 166.7, 147.8, 143.6, 137.5, 136.0, 134.5, 130.8, 129.9, 127.0, 125.3, 124.1, 120.5, 115.5, 112.0, 46.4, 31.4, 21.1. HRMS (ESI): calcd for $\text{C}_{22}\text{H}_{19}\text{N}_3\text{O}_3\text{S}_2$ $[\text{M} + \text{H}]^+$ 438.0934, found 438.0926.

4.2.28. *(Z)-2-(5-((5-chloro-1-(2-fluorobenzyl)-1H-benzo[d]imidazol-2-yl)methylene)-4-oxo-2-thioxothiazolidin-3-yl)acetic acid (11a)*. Rhodanine-3-acetic acid and **7a** were used as reactants to give **11a**. Yellow solid, yield: 71%, mp: 296.4–298.1 °C. ^1H NMR (400 MHz, DMSO- d_6) δ 13.50 (s, 1H), 8.02 (s, 1H), 7.94 (d, J = 1.8 Hz, 1H), 7.74 (d, J = 8.8 Hz, 1H), 7.42 (dd, J = 8.8, 2.0 Hz, 1H), 7.40 – 7.34 (m, 1H), 7.27 – 7.22 (m, 1H), 7.19 – 7.10 (m, 2H), 5.95 (s, 2H), 4.75 (s, 2H). ^{13}C NMR (101 MHz, DMSO- d_6) δ 198.1, 167.8, 166.3, 160.49 (d, J = 245.9 Hz), 149.2, 144.1, 134.7, 131.1, 130.8 (d, J = 8.2 Hz), 129.6 (d, J = 3.8 Hz), 128.7,

125.5 (d, $J = 3.4$ Hz), 123.9 (d, $J = 14.5$ Hz), 119.8, 116.4, 116.2, 113.5, 45.3, 42.0 (d, $J = 3.4$ Hz). HRMS (ESI): calcd for $C_{20}H_{13}ClFN_3O_3S_2$ [$M + H$]⁺ 462.0142, found 462.0131.

4.2.29. *(Z)-2-(5-((6-chloro-1-(2-fluorobenzyl)-1H-benzo[d]imidazol-2-yl)methylene)-4-oxo-2-thioxothiazolidin-3-yl)acetic acid (11b)*. Rhodanine-3-acetic acid and **7b** were used as reactants to give **11b**. Yellow solid, yield: 76%, mp: 288.7–290.1 °C. ¹H NMR (400 MHz, DMSO-*d*₆) δ 13.48 (s, 1H), 7.98 (s, 1H), 7.90 (d, $J = 1.8$ Hz, 1H), 7.87 (d, $J = 8.7$ Hz, 1H), 7.41 – 7.36 (m, 2H), 7.28 – 7.22 (m, 1H), 7.20 – 7.10 (m, 2H), 5.94 (s, 2H), 4.75 (s, 2H). ¹³C NMR (101 MHz, DMSO-*d*₆) δ 198.1, 167.8, 166.3, 160.48 (d, $J = 246.0$ Hz), 148.9, 142.1, 136.6, 130.8, 129.9, 129.5 (d, $J = 3.8$ Hz), 125.4 (d, $J = 3.3$ Hz), 124.4, 123.8 (d, $J = 14.6$ Hz), 121.9, 116.2, 111.9, 45.3, 41.9 (d, $J = 2.9$ Hz). HRMS (ESI): calcd for $C_{20}H_{13}ClFN_3O_3S_2$ [$M + H$]⁺ 462.0142, found 462.0137.

4.2.30. *(Z)-2-(5-((5-fluoro-1-(2-fluorobenzyl)-1H-benzo[d]imidazol-2-yl)methylene)-4-oxo-2-thioxothiazolidin-3-yl)acetic acid (11c)*. Rhodanine-3-acetic acid and **7c** were used as reactants to give **11c**. Yellow solid, yield: 77%, mp: 292.4–293.6 °C. ¹H NMR (400 MHz, DMSO-*d*₆) δ 13.47 (s, 1H), 8.01 (s, 1H), 7.73 (dd, $J = 9.0, 4.7$ Hz, 1H), 7.68 (dd, $J = 9.5, 2.3$ Hz, 1H), 7.39 – 7.35 (m, 1H), 7.31 – 7.21 (m, 2H), 7.18 – 7.10 (m, 2H), 5.94 (s, 2H), 4.75 (s, 2H). ¹³C NMR (101 MHz, DMSO-*d*₆) δ 198.1, 167.8, 166.3, 160.6 (d, $J = 240.6$ Hz), 160.5 (d, $J = 246.0$ Hz), 148.8 (d, $J = 3.1$ Hz), 140.2, 136.4 (d, $J = 14.0$ Hz), 130.9 (d, $J = 8.1$ Hz), 123.0, 129.6 (d, $J = 3.8$ Hz), 125.4 (d, $J = 3.4$ Hz), 123.7 (d, $J = 14.6$ Hz), 122.0 (d, $J = 10.3$ Hz), 116.4, 116.2, 112.9 (d, $J = 25.7$ Hz), 98.4 (d, $J = 28.1$ Hz), 45.2, 41.9 (d, $J = 2.6$ Hz). HRMS (ESI): calcd for $C_{20}H_{13}F_2N_3O_3S_2$ [$M + H$]⁺ 446.0471, found 446.0438.

4.2.31. *(Z)-2-(5-((6-fluoro-1-(2-fluorobenzyl)-1H-benzod[*j*]imidazol-2-yl)methylene)-4-oxo-2-thioxothiazolidin-3-yl)acetic acid (11d).* Rhodanine-3-acetic acid and **7d** were used as reactants to give **11d**. Yellow solid, yield: 83%, mp: 275.4–277.3 °C. ¹H NMR (400 MHz, DMSO-*d*₆) δ 13.46 (s, 1H), 7.97 (s, 1H), 7.90 – 7.86 (m, 1H), 7.64 (dd, *J* = 9.2, 2.3 Hz, 1H), 7.39 – 7.34 (m, 1H), 7.28 – 7.20 (m, 2H), 7.18 – 7.11 (m, 2H), 5.91 (s, 2H), 4.74 (s, 2H). ¹³C NMR (101 MHz, DMSO-*d*₆) δ 198.2, 167.8, 166.3, 160.5 (d, *J* = 245.9 Hz), 159.9 (d, *J* = 237.9 Hz), 149.3, 143.6 (d, *J* = 13.3 Hz), 132.6, 130.8 (d, *J* = 8.4 Hz), 130.6, 129.6 (d, *J* = 3.8 Hz), 125.4 (d, *J* = 3.3 Hz), 123.8 (d, *J* = 14.5 Hz), 116.4, 116.2, 113.9 (d, *J* = 26.6 Hz), 113.1 (d, *J* = 10.1 Hz), 105.9 (d, *J* = 24.2 Hz), 45.2, 41.9 (d, *J* = 3.1 Hz). HRMS (ESI): calcd for C₂₀H₁₃F₂N₃O₃S₂ [M + H]⁺ 446.0451, found 446.0442.

4.2.32. *(Z)-2-(5-((1-(2-fluorobenzyl)-5-methoxy-1H-benzod[*j*]imidazol-2-yl)methylene)-4-oxo-2-thioxothiazolidin-3-yl)acetic acid (11e).* Rhodanine-3-acetic acid and **7e** were used as reactants to give **11e**. Yellow solid, yield: 80%, mp: 278.8–280.2 °C. ¹H NMR (400 MHz, DMSO-*d*₆) δ 13.46 (s, 1H), 7.99 (s, 1H), 7.58 (d, *J* = 9.0 Hz, 1H), 7.38 – 7.32 (m, 2H), 7.26 – 7.21 (m, 1H), 7.15 (t, *J* = 7.4 Hz, 1H), 7.09 – 7.05 (m, 1H), 7.01 (dd, *J* = 9.0, 2.3 Hz, 1H), 5.89 (s, 2H), 4.74 (s, 2H), 3.83 (s, 3H). ¹³C NMR (101 MHz, DMSO-*d*₆) δ 198.4, 167.8, 166.4, 160.4 (d, *J* = 245.8 Hz), 157.4, 147.7, 144.5, 130.7 (d, *J* = 8.2 Hz), 129.5 (d, *J* = 3.8 Hz), 129.1, 125.4 (d, *J* = 3.4 Hz), 124.1 (d, *J* = 14.5 Hz), 116.7, 116.5, 116.1 (d, *J* = 20.9 Hz), 112.6, 101.6, 56.1, 45.2, 41.7 (d, *J* = 3.2 Hz). HRMS (ESI): calcd for C₂₁H₁₆FN₃O₄S₂ [M + H]⁺ 458.0619, found 458.0623.

4.2.33. *(Z)-2-(5-((1-(2-fluorobenzyl)-6-methoxy-1H-benzod[*j*]imidazol-2-yl)methylene)-4-oxo-2-thioxothiazolidin-3-yl)acetic acid (11f).* Rhodanine-3-acetic acid and **7f** were used as

reactants to give **11f**. Yellow solid, yield: 91%, mp: 283.4–285.1 °C. ¹H NMR (400 MHz, DMSO-*d*₆) δ 13.44 (s, 1H), 7.91 (s, 1H), 7.74 (d, *J* = 8.9 Hz, 1H), 7.38 – 7.34 (m, 1H), 7.29 – 7.23 (m, 2H), 7.15 (t, *J* = 7.6, 0.8 Hz, 1H), 7.03 (t, *J* = 7.7, 1.2 Hz, 1H), 6.99 (dd, *J* = 8.9, 2.3 Hz, 1H), 5.90 (s, 2H), 4.73 (s, 2H), 3.81 (s, 3H). ¹³C NMR (101 MHz, DMSO-*d*₆) δ 198.2, 167.8, 166.3, 160.4 (d, *J* = 245.6 Hz), 158.5, 147.0, 138.5, 137.0, 130.7 (d, *J* = 8.0 Hz), 128.0, 125.4 (d, *J* = 3.4 Hz), 124.1 (d, *J* = 14.6 Hz), 121.4, 116.8, 116.1 (d, *J* = 20.7 Hz), 114.9, 94.3, 56.2, 45.2, 41.4 (d, *J* = 3.5 Hz). HRMS (ESI): calcd for C₂₁H₁₆FN₃O₄S₂ [M + H]⁺ 458.0619, found 458.0626.

4.2.34. (Z)-5-((1-(2-fluorobenzyl)-1H-benzodjimidazol-2-yl)methylene)-2-

thioxothiazolidin-4-one (11g). Rhodanine and **5j** were used as reactants to give **11g**. Yellow solid, yield: 90%, mp: 258.4–260.1 °C. ¹H NMR (400 MHz, DMSO-*d*₆) δ 13.81 (s, 1H), 7.89 – 7.61 (m, 3H), 7.27 (m, 4H), 7.19 – 6.98 (m, 2H), 5.88 (s, 2H). ¹³C NMR (101 MHz, DMSO-*d*₆) δ 200.7, 169.2, 160.4 (d, *J* = 245.8 Hz), 148.0, 143.5, 135.8, 133.9, 130.7 (d, *J* = 8.1 Hz), 129.5 (d, *J* = 3.6 Hz), 125.8.6, 125.3 (d, *J* = 3.2 Hz), 124.1 (d, *J* = 14.5 Hz), 120.4, 116.1 (d, *J* = 20.9 Hz), 114.6, 111.8, 41.6 (d, *J* = 3.3 Hz). HRMS (ESI): calcd for C₁₄H₁₂FN₃OS₂ [M + H]⁺ 370.0418, found 370.0432.

4.2.35. (Z)-3-(5-((1-(2-fluorobenzyl)-1H-benzodjimidazol-2-yl)methylene)-4-

oxo-2-thioxothiazolidin-3-yl)propanoic acid (11h). Rhodanine-3-propanoic and **5j** were used as reactants to give **11h**. Yellow solid, yield: 86%, mp: 258.4–260.1 °C. ¹H NMR (400 MHz, DMSO-*d*₆) δ 12.51 (s, 1H), 7.94 (s, 1H), 7.85 – 7.81 (m, 1H), 7.68 (d, *J* = 7.5 Hz, 1H), 7.39 – 7.31 (m, 3H), 7.27 – 7.22 (m, 1H), 7.14 (t, *J* = 7.4 Hz, 1H), 7.06 (t, *J* = 7.0 Hz, 1H), 5.92 (s, 2H), 4.26 – 4.20 (m, 2H), 2.68 – 2.62 (m, 2H). ¹³C NMR (101 MHz, DMSO-*d*₆) δ 198.4,

172.2, 166.7, 160.4 (d, $J = 245.9$ Hz), 148.0, 143.5, 135.8, 131.00, 130.8 (d, $J = 8.2$ Hz), 129.6 (d, $J = 3.5$ Hz), 125.4 (d, $J = 7.2$ Hz), 124.1, 120.5, 116.1 (d, $J = 20.9$ Hz), 115.6, 111.9, 41.6, 41.5, 31.4. HRMS (ESI): calcd for $C_{21}H_{16}FN_3O_3S_2$ $[M + H]^+$ 442.0617, found 442.0623.

4. 3. Biological evaluation

4.3.1. *Topo I inhibitory activity*

In this relaxation assay, pBR322 plasmid (TaKaRa, Kyoto, Japan) was used to determine the effects of the synthesized compounds on DNA relaxation catalytic by Topo I (TaKaRa, Kyoto, Japan) by using camptothecin as a positive control. The reaction mixture was prepared according to the literature with minor modifications, and incubated at 37 °C for 30 min. The reactions were terminated by the addition of dye solution containing 1% SDS, 0.02% bromophenol blue and 50% glycerol. The mixtures were applied to 1% agarose gel and subjected to electrophoresis for 1.5 h, in 1×TAE buffer (40 mM Tris-acetate, 2 mM EDTA). Gels were stained for 30 min in an aqueous solution of Ged Red ($0.5 \mu\text{g}\cdot\text{ml}^{-1}$). DNA bands were visualized by transillumination with UV light and then photographed with an Alpha Innotech digital imaging system⁶.

4.3.2. *Topo I-mediated DNA unwinding assay*

Relaxed pBR322 DNA plasmid utilized in this unwinding assay was generated by treating pBR322 with Topo I in the reaction buffer (50 mM Tris-HCl, pH 7.5, 50 mM KCl, 10 mM MgCl_2 , 0.5 mM DTT, 0.1 mM EDTA, and $30 \mu\text{g}\cdot\text{ml}^{-1}$ BSA) prior to the addition of other components. Assay mixtures is composed of 0.1 μg relaxed pBR322 DNA, Topo I (4 U), and the tested compounds in 20 μL Topo I reaction buffer. Following a 10 min incubation of DNA and drugs at room temperature, Topo I (1 U) was added, and the reaction were incubated at

37 °C for 30 min. An equal volume of phenol chloroform was added to stop the reaction. Aqueous samples (20 µL) were removed from the reaction, and 3 µL of stop solution (0.77% SDS, 77 mmol NaEDTA, pH 8.0) followed by 2 µL of agarose gel loading buffer was added to each sample. Samples were subjected to electrophoresis in 1×TAE buffer (40 mM Tris-acetate, 2 mM EDTA). DNA bands were visualized by transillumination with UV light and then photographed with an Alpha Innotech digital imaging system⁸.

4.3.3. *Topo II inhibitory activity*

Relaxation assay were carried out according to the manufacturer's instructions with minor modifications. The reaction mixture containing 200 ng of pBR322 DNA plasmid and 1 U of Topo II (TopoGEN) was incubated in the presence or absence of the synthesized compounds in a final volume of 20 µL in Topo II reaction buffer (50 mM Tris-HCl, pH 8.0, 150 mM NaCl, 10 mM MgCl₂, 2 mM ATP, 0.5 mM DTT, and 30 µg·mL⁻¹ BSA). The mixture was incubated for 30 min at 37 °C and was terminated with 6× stop buffer (5 µL per 20 µL reaction volume). Stop buffer contained 5% sarcosyl, 0.02% bromophenol blue, and 25% glycerol. Reaction products were analyzed on a 1% agarose gel and electrophoresis in TAE buffer (40 mM Tris-acetate and 2 mM EDTA) for 1.5 h at 75 V. Gels were stained for 30 min in an aqueous solution of Ged Red (0.5 µg·mL⁻¹). DNA bands were visualized through transillumination with UV light and then photographed with an Alpha Innotech digital imaging system¹⁶.

4.3.4. *Topo II-mediated DNA cleavage reaction assay*

In brief, Topo II (6 U), 0.1 µg of pBR322 DNA, and 50 µM synthesized compounds (or etoposide, 100 µM) were employed in a total of 20 µL of Topo II buffer (50 mM Tris-HCl, pH 8.0, 150 mM NaCl, 10 mM MgCl₂, 2 mM ATP, 0.5 mM DTT, and 30 µg·mL⁻¹ BSA). After

incubating for 6 min at 37 °C to reach the cleavage religation equilibrium, cleavage intermediates were trapped by adding 2 μL of 1% SDS, followed by 2 μL of 250 mM NaEDTA at pH 8.0. Proteinase K was added (2 μL of 0.8 $\text{mg}\cdot\text{mL}^{-1}$), and reactions were incubated for 30 min at 45 °C to digest the Topo II. Samples were mixed with 2 μL of agarose gel loading buffer (30% sucrose, 0.5% bromophenol blue, and 0.5% xylene cyanole FF in 10 mM Tris-HCl, pH 7.9), heated at 72 °C for 2 min, and subjected to electrophoresis in a 1% agarose gel in TAE buffer (40 mM Tris-acetate and 2 mM EDTA) for 1 h at 75 V. Gels were stained for 30 min in an aqueous solution of Ged Red (0.5 $\mu\text{g}\cdot\text{mL}^{-1}$) and kept on electrophoresis for 30-45 min at 75 V. Cleavage was monitored by the conversion of negatively supercoiled plasmid to nicked DNA. DNA bands were visualized by UV light and photographed with an Alpha Innotech digital imaging system¹⁶.

4.3.5. MTT assay

Briefly, the cells were plated at a density of 5000 per well in 96-well microplates and allowed to incubate over night. The compounds were added to the wells at increasing concentrations (0-50 μM). After 48 h, each well was treated with 20 μL MTT (2.5 $\text{mg}\cdot\text{mL}^{-1}$) solution, and the cells were further incubated at 37 °C for 4 h. At the end of the incubation, the untransformed MTT was removed, and 100 μL of DMSO was added. The microplates were well shaken to dissolve the formazan dye, and the absorbance at 570 nm was measured using a microplate reader (Bio-Tek)²⁹.

References

- [1] C. Bailly, *Chem. Rev.*, 2012, **112**, 3611–3640.
- [2] Y. Pommier, *ACS Chem. Biol.*, 2013, **8**, 82–95.
- [3] Y. Pommier, Y. Sun, S.N. Huang, J.L. Nitis, *Nat. Rev. Mol. Cell. Biol.*, 2016, **17**, 703–721.
- [4] G. Capranico, J. Marinello, G. Chillemi, *J. Med. Chem.*, 2017, **60**, 2169–2192.

- [5] J.L. Nitiss, *Nat. Rev. Cancer*, 2009, **9**, 338–350.
- [6] M.S. Christodoulou, M. Zarate, F. Ricci, G. Damia, S. Pieraccini, F. Dapiaggi, M. Sironi, L. Lo Presti, A.N. García-Argaez, L. Dalla Via, D. Passarella, *Eur. J. Med. Chem.*, 2016, **118**, 79–89.
- [7] M.S. Christodoulou, F. Calogero, M. Baumann, A.N. García-Argaez, S. Pieraccini, M. Sironi, F. Dapiaggi, R. Bucci, G. Broggin, S. Gazzola, S. Liekens, A. Silvani, M. Lahtela-Kakkonen, N. Martinet, A. Nonell-Canals, E. Santamaría-Navarro, I. R. Baxendale, D. Dalla Via, D. Passarella, *Eur. J. Med. Chem.*, 2015, **92**, 766–775.
- [8] B.L. Yao, Y.W. Mai, S.B. Chen, H.T. Hua, P.F. Yao, T.M. Ou, J.H. Tan, H.G. Wang, D. Li, S.L. Huang, L.Q. Gu, Z.S. Huang, *Eur. J. Med. Chem.*, 2015, **92**, 540–553.
- [9] S.T. Zhuo, C.Y. Li, M.H. Hu, S.B. Chen, P.F. Yao, S.L. Huang, T.M. Ou, J.H. Tan, L.K. An, D. Li, Z.S. Huang, *Org. Biomol. Chem.*, 2013, **11**, 3989–4005.
- [10] J.A. Ortega, L. Riccardi, E. Minniti, M. Borgogno, J. M. Arencibia, M. L. Greco, A. Minarini, C. Sissi, M.D. Vivo, *J. Med. Chem.*, 2018, **61**, 1375–1379.
- [11] Z.Z. Chen, S.Q. Li, W.L. Liao, Z.G. Xie, M.S. Wang, Y. Cao, J. Zhang, Z.G. Xu, *Tetrahedron*, 2015, **71**, 8424–8427.
- [12] W.A. M.F. Khan, G. Verma, M. Shaquiquzzaman, M.A. Rizvi, S.H. Mehdi, M. Akhter, M. Mumtaz-Alam, *Eur. J. Med. Chem.*, 2017, **106**, 705–753.
- [13] A.T. Baviskar, C. Madaan, R. Preet, P. Mohapatra, V. Jain, A. Agarwal, S.K. Guchhait, C.N. Kundu, U.C. Banerjee, P.V. Bharatnam, *J. Med. Chem.*, 2011, **54**, 5013–5030.
- [14] A.T. Baviskar, S.M. Amrutkar, N. Trivedi, V. Chaudhary, A. Nayak, S.K. Guchhait, U.C. Banerjee, P.V. Bharatam, C.N. Kundu, *ACS Med. Chem. Lett.*, 2015, **6**, 481–485.
- [15] G. Priyadarshani, A. Nayak, S.M. Amrutkar, S. Das, S.K. Guchhait, C.N. Kundu, U.C. Banerjee, *ACS Med. Chem. Lett.*, 2016, **7**, 1056–1061.
- [16] P.H. Li, P. Zeng, S.B. Chen, P.F. Yao, Y.W. Mai, J.H. Tang, T.M. Ou, S.L. Huang, D. Li, L.Q. Gu, Z.S. Huang, *J. Med. Chem.*, 2016, **59**, 238–252.
- [17] T. Mendgen, C. Steuer, C.D. Klein, *J. Med. Chem.*, 2012, **55**, 743–753.
- [18] S.Q. Tang, Y.Y.I. Lee, D.S. Packiaraj, H.K. Ho, C.L.L. Chai, *Chem. Res. Toxicol.*, 2015, **28**, 2019–2023.
- [19] D. Kaminsky, A. Kryshchshyn, R. Lesyk, *Expert Opin Drug Discov.*, 2017, **12**, 1233–1252.
- [20] P.H. Li, H. Jiang, W.J. Zhang, Y.L. Li, M.C. Zhao, W. Zhou, L.Y. Zhang, Y.D. Tang, C.Z. Dong, Z.S. Huang, H.X. Chen, Z.Y. Du, *Eur. J. Med. Chem.*, 2018, **145**, 498–510.
- [21] C. Li, J.C. Liu, Y.R. Li, C. Gou, M.L. Zhang, H.Y. Liu, X.Z. Li, C.J. Zheng, H.R. Piao, *Bioorg. Med. Chem. Lett.*, 2015, **25**, 3052–3056.
- [22] D.D. Shubedar, M.H. Shaikh, B.B. Shigate, L. Nawale, D. Sarkar, V.M. Khedar, V.M. Khedar, F.A.K. Khan, J.N. Sangshetti, *Eur. J. Med. Chem.*, 2017, **125**, 385–399.
- [23] H. Fu, X. Hou, L. Wang, Y. Dun, X. Yang, H. Fang, *Bioorg. Med. Chem. Lett.*, 2015, **25**, 5265–5269.
- [24] M. Azizmohammadi, M. Khoobi, A. Ramazani, S. Emami, A. Zarrin, O. Firuzi, R. Miri, A. Shafiee, *Eur. J. Med. Chem.*, 2013, **59**, 15–22.
- [25] I. Hueso-Falcón, Á. Amesty, L. Anaissi-Afonso, I. Lorenzo-Castrillejo, F. Machín, A. Estévez-Braun, *Bioorg. Med. Chem. Lett.*, 2017, **27**, 484–489.
- [26] S.Y. Tan, D.H. Sun, J. K. Lyu, X. Sun, F.S. Wu, Q. Li, Y.Q. Yang, J.X. Liu, X. Wang, Z.

- Chen, H.L. Li, X.H. Qian, Y.F. Xu, *Bioorg. Chem. Med.*, 2015, **23**, 5672–5680.
- [27] H. Sun, G. Tawa, A. Wallqvist, *Drug Discovery Today*, 2012, **17**, 310–324.
- [28] C. Shu, H. Ge, M. Song, J.H. Chen, H. Zhou, Q. Qi, F. Wang, X. Ma, X. Yang, G. Zhang, Y. Ding, D. Zhou, P. Peng, C.K. Shih, J. Xu, F. Wu, *ACS Med. Chem. Lett.*, 2014, **5**, 921–926.
- [29] H. Jiang, W.J. Zhang, P.H. Li, C.Z. Dong, K. Zhang, H.X. Chen, Z.Y. Du, *Bioorg. Med. Chem. Lett.*, 2018, **28**, 1320–1323
- [30] R.B. Wang, C.S. Chen, X.J. Zhang, C.D. Zhang, Q. Zhong, G.L. Chen, Q. Zhang, S.L. Zheng, G.D. Wang, Q.H. Chen, *J. Med. Chem.*, 2015, **58**, 4713–4726.
- [31] M.X. Song, C.J. Zhang, X.Q. Deng, Q. Wang, S.P. Hou, T.T. Liu, X.L. Xing, H.R. Xiao, *Eur. J. Med. Chem.*, 2012, **54**, 403–412.
- [32] S. Classen, S. Olland, J. M. Berger, *Proc. Natl. Acad. Sci. U. S. A.* 2003, **100**, 10629–10634.
- [33] H. Wei, A. J. Ruthenburg, S. K. Bechis, G. L. Verdine, *J. Biol. Chem.* 2005, **280**, 37041–37047.

Figure and Scheme Captions

Fig. 1. Design of novel agents as potential Topo II-targeting anticancer agents.

Fig. 2. Chemical structure of the target compounds.

Fig. 3. Agarose gel assay for Topo II inhibition by the synthesized compounds. (A, B, C, and D), lane D, pBR322 DNA; lane T, pBR322 DNA + Topo II; lane E, pBR322 DNA + Topo II + etoposide (100 μ M); other lanes, pBR322 DNA + Topo II + the synthesized compounds.

Fig. 4. Topo I inhibitory activity of the synthesized compounds. (A), (B), (C) and (D) lane D: pBR322 DNA; lane T: pBR322 DNA + Topo I; lane C: pBR322 DNA + Topo I + camptothecin (100 μ M); other lanes: pBR322 DNA + Topo I + the synthesized compounds (50 μ M).

Fig. 5. (A) Effects of compounds **8g** and **8j** on Topo II mediated DNA cleavage complexes formation. Lanes 1-2: control group of supercoiled pBR322 DNA without or with Topo II; lanes 3-5, effects of etoposide (100 μ M) and tested compound (50 μ M) on Topo II with DNA. Lanes 6-7, pretreatment of tested compounds (50 μ M) antagonizes the etoposide (100 μ M)-enhanced DNA cleavage. The positions of supercoiled DNA (S), relaxed DNA (R),

linear DNA (L), and nicked DNA (N) are indicated. (B) The unwinding capacity of **8g** and **8j**. Lane D, pBR322 DNA; lane T, pBR322 DNA + Topo I; other lane, pBR322 DNA + Topo I + **8g**, **8j**, or EB at different concentration.

Fig. 6. Schematic representation of the proposed binding modes of **8g** and **8j** with the catalytic site of the ATPase domain of Topo II (PDB code:1ZXM) (A, compound **8g**; B, compound **8j**).

Scheme 1. Synthesis rout of the target compounds. Reagents and conditions (a) glycolic acid, 4N HCl, 100 °C, 6 h; (b) DMF, appropriate benzyl bromide, bromoethane or 2-bromo-1-phenylethanone, K₂CO₃, rt, 24 h; (c) DCM, Dess-Martin reagent, 4 °C, 1 h; (d) Rhodanine moiety, NaOAc, acetic acid, 110 °C, 4 h.

Table 1. Cytotoxic activity and Topo II inhibition potency of the synthesized compounds

Cpd.	IC ₅₀ (mean ± SD) ^a (μM)						Topo II Inhibition ^b
	Hela	HL-60	MDA-MB-201	Raji	PC-3	A549	
8a	12.94 ±3.43	0.87±0.20	8.72±2.44	1.19±0.24	8.49±2.38	9.12±3.17	+
8b	>50	6.42±1.72	28.36±5.62	11.37±2.20	21.12±4.63	27.31±5.72	-
8c	16.31 ±4.25	7.64±0.89	11.24±3.16	9.78±3.14	14.42±3.25	26.58±5.43	-
8d	18.57 ±4.05	5.32±1.25	7.76±2.25	2.51±0.62	8.27±2.28	11.42±3.16	-
8e	13.92 ±3.47	1.42±0.46	2.62±0.82	1.77±0.34	4.86±1.23	3.57±1.24	++
8f	22.66 ±4.62	0.96±0.24	1.82±0.57	3.86±1.12	10.79±2.42	8.76±2.68	+

8g	1.28 ±0.23	0.54±0.18	1.04±0.26	0.96±0.31	2.64±0.85	3.22±1.26	++
8h	8.72 ±1.21	2.65±0.73	5.58±1.25	11.42±2.89	9.67±2.33	17.51±3.69	++
8i	21.42 ±5.02	3.56±0.94	12.46±3.82	18.83±4.26	22.86±5.61	25.28±6.75	++
8j	0.64 ±0.12	0.21±0.13	0.33±0.16	1.23±0.35	1.86±0.53	2.67±0.89	++
8k	26.12 ±5.46	6.52±1.16	11.48±4.28	8.96±1.78	21.68±5.47	12.83±3.56	-
8l	>50	7.21±2.49	22.46±5.28	13.28±3.46	35.71±6.55	23.16±6.58	-
8m	15.98 ±3.42	2.74±0.74	3.76±1.51	7.25±2.76	5.97±1.69	13.42±3.63	+
8n	17.69 ±4.04	1.41±0.53	1.28±0.53	2.11±0.76	6.37±1.61	5.17±1.52	++
8o	3.52 ±0.78	2.12±0.23	1.88±0.72	5.56±1.38	3.25±1.12	9.44±2.41	-
9a	14.79 ±3.03	3.96±0.73	6.31±2.18	8.24±2.21	9.87±2.34	12.77±3.60	++
9b	26.68 ±6.21	5.44±1.03	12.86±4.12	6.32±1.78	8.75±2.24	5.15±1.66	-
9c	27.26 ±5.87	2.43±0.56	1.12±0.56	3.18±1.16	6.45±1.40	9.85±3.11	++
9d	27.41±5.71	15.88±3.26	16.85±4.18	12.28±3.56	8.75±1.79	9.46±2.17	++
10a	21.44 ±1.96	2.72±0.69	13.72±4.58	20.88±4.52	26.71±6.32	38.61±5.13	++
10b	10.96 ±1.82	2.84±0.91	3.96±1.27	2.79±0.86	1.52±0.36	9.97±3.16	++
10c	2.38 ±1.22	1.17±0.43	6.55±2.13	3.28±1.37	10.24±2.79	13.82±4.41	++
10d	3.92 ±0.77	1.69±0.83	3.86±1.35	2.44±0.77	5.82±1.75	9.64±2.79	++
10e	1.82 ±0.56	0.77±0.25	1.22±0.54	1.79±0.53	3.64±1.08	5.68±1.84	++
10f	6.44 ±0.98	1.92±0.58	3.77±1.28	10.76±2.67	16.17±4.84	23.61±4.59	++
10g	25.25 ±5.20	2.66±0.83	6.42±1.22	4.48±1.23	9.78±2.46	5.31±1.66	+
10h	11.2 ±1.82	4.14±0.79	3.79±1.68	6.68±1.28	9.31±2.75	8.74±2.43	-
11a	9.52 ±1.08	0.87±0.23	1.67±0.73	2.78±0.98	3.48±1.62	5.64±1.99	++
11b	7.62 ±0.93	5.23±1.33	9.57±3.62	8.87±1.89	17.31±4.81	26.86±5.76	++
11c	>50	>50	22.44±5.38	20.42±4.21	>50	32.65±6.48	-
11d	>50	5.23±1.26	>50	22.37±5.28	>50	>50	+
11e	22.48±2.91	3.41±1.03	16.92±4.76	11.46±3.68	24.71±5.88	18.35±4.87	-
11f	28.13±3.62	6.44±1.73	22.44±7.68	12.35±3.28	>50	36.18±9.45	++
11g	36.11±7.72	8.42±2.13	21.33±5.38	25.48±5.57	>50	>50	+
11h	26.52±0.98	5.72±1.67	9.53±2.71	11.27±3.62	28.61±5.32	18.73±4.28	-
Etoposide	28.61±3.98	0.58±0.11	30.28±5.41	1.21±0.24	13.18±3.65	2.46±0.67	++
Camptothecin	>50	0.42±0.19	16.44±4.86	3.27±1.21	18.24±4.53	2.21±0.58	n.d. ^c

^aEach assay was performed in quadruplicate with the number of determinations $N > 2$, and the results are expressed in mean value, where the IC_{50} means the concentration of drug needed to reduce the cell number to 50%.

^bThe relative Topo II inhibitory potencies of the synthesized compounds are present as follows: -, no detectable activity at 20 μ M ; +, weak activity at 20 μ M ; ++, strong activity at 20 μ M.

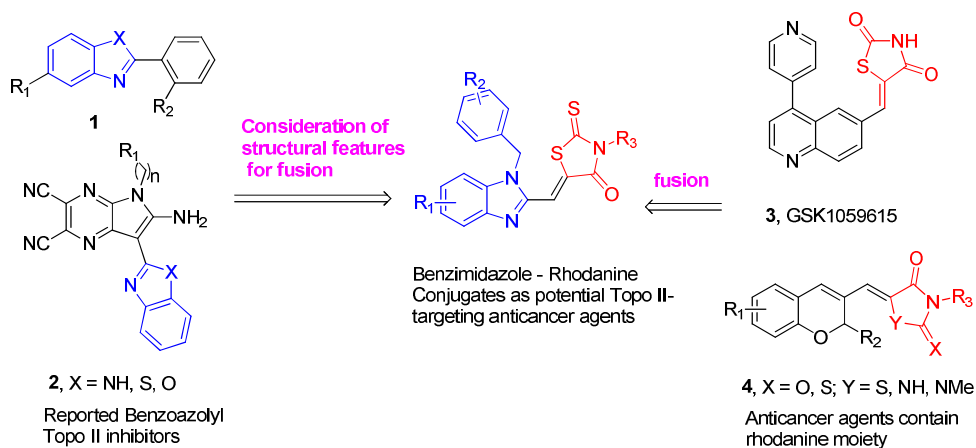


Fig. 1

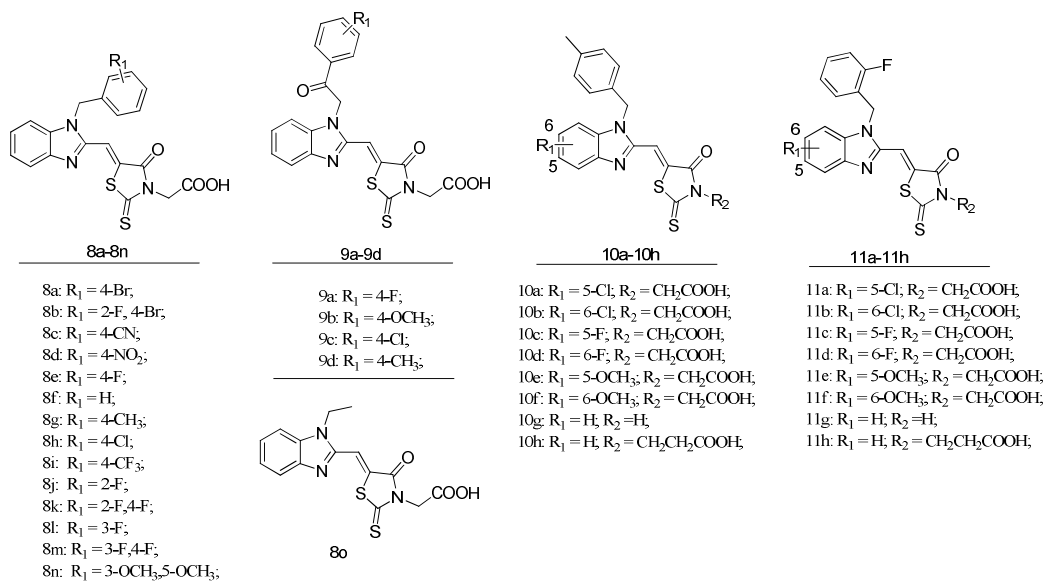


Fig. 2

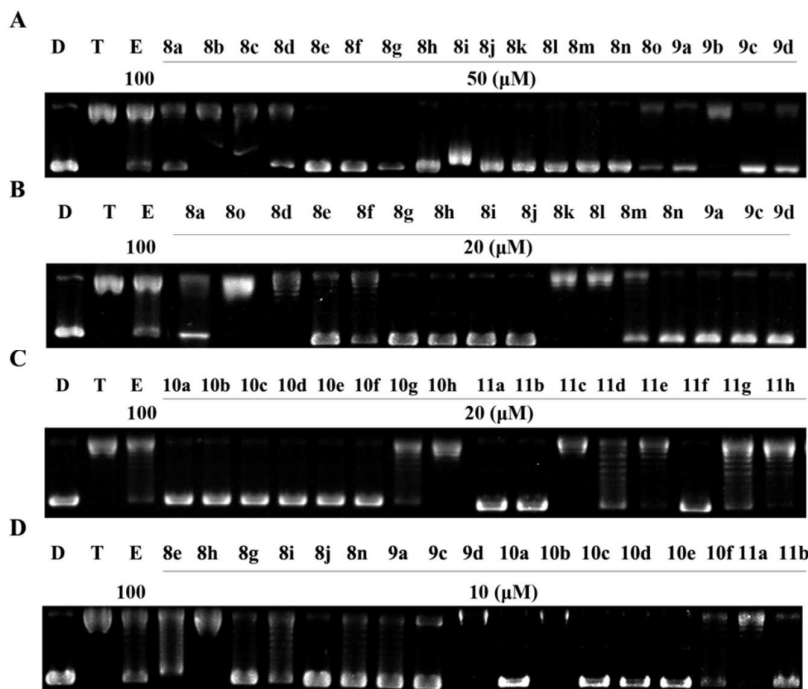


Fig. 3

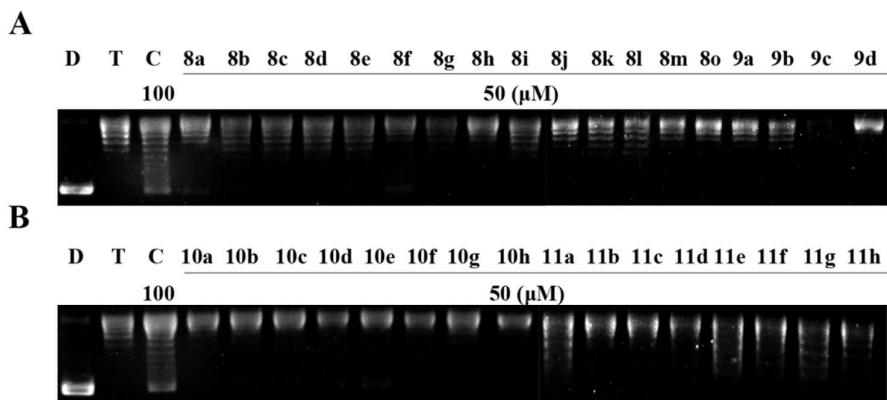


Fig. 4

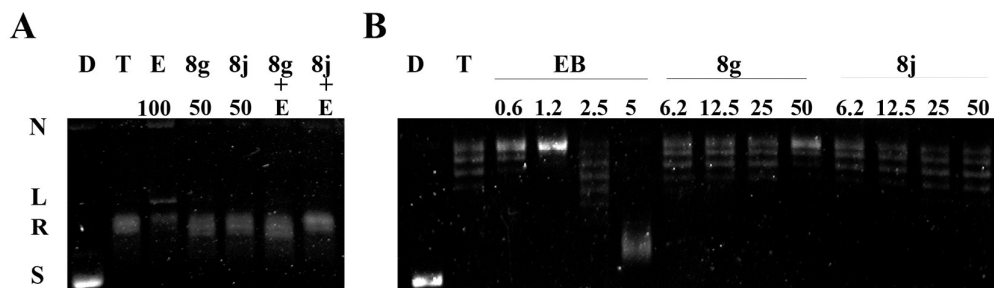


Fig. 5

MedChemComm Accepted Manuscript

